Proceedings of ASME 2010 4th International Conference on Energy Sustainability
ES2010
May 17-22, 2010 Phoenix, Arizona, USA

ES2010-90378

A COMPARATIVE WIND INVESTIGATION USING MESOSCALE NUMERICAL PREDICTIONS AND EXPERIMENTAL DATA AT AUBREY CLIFFS, ARIZONA

Michael S. Barton
M.S. Candidate in Mechanical Engineering, Northern Arizona University
Flagstaff, Arizona USA
Michael.Barton1@gmail.com

Thomas L. Acker
Professor of Mechanical Engineering, Northern Arizona University
Flagstaff, Arizona USA
Tom.Acker@nau.edu

Earl P.N. Duque
Manager of Applied Research
Intelligent Light
Rutherford, New Jersey USA
EPD@ilight.com

ABSTRACT

The purpose of this paper is to demonstrate the validity of mesoscale numerical weather prediction modeling near the complex terrain at Aubrey Cliffs, Arizona, and to investigate the influence of the outer domain size employed on the computational results. Mesoscale Modeling v5 (MM5) was implemented to produce numerical wind data that was compared with experimental wind data. The results obtained from the analysis show that MM5 predicts the wind flow near the Aubrey Cliffs accurately. In addition to predicting the wind speed and direction, the wind power density at the site was also computed. A three month MM5 simulation was completed for the proposed site, with a grid resolution of 1-km in the proximity of the cliffs. Two different gridding scenarios were used to investigate the accuracy of the numerical results and the effect outermost modeling domain. It was found that the model predicts the average wind speed at the site within 4% of the actual observed values. It was also determined that the MM5 model does not require an extended radius of influence to correctly determine the wind speed.

INTRODUCTION

One major aspect that concerns the development of a particular site for wind energy is adequate knowledge of long term wind characteristics. Multiple years of quantitative are desired for analysis to determine the feasibility of a given site. The accuracy of this data is extremely important to the wind developer so they may properly assess the potential financial outcomes from the wind energy production (1). Acquiring accurate wind data, especially in complex terrain, can be complicated and may require the use of different measuring techniques. Novel approaches to measuring the wind and understanding atmospheric flow conditions have been developed in recent years. Some methods include:

- A number of different physical wind measurements devices, including; cup anemometers, sonic anemometers, SODAR, and LIDAR (2).
- Direct use of Mesoscale Modeling v5 (MM5) (3).
- Altering MM5 results with model output statistical modules (4).
- Coupling MM5 results or physical wind measurements to Wind Atlas Analysis and Application Program (WAsP) (5), (6).
- Combining numerical weather prediction (NWP) models with computational fluid dynamics (CFD) (7).

Similar studies have been conducted by private entities in the process of developing wind power plants and currently take place all over the world. All current wind developers directly measure the wind using meteorological towers as a part of their site investigation. Most meteorological towers are equipped with anemometers, wind vanes, temperature sensors, and pressure sensors that record averaged data every 10-minutes (8). Due to the length of time needed to acquire physical data (minimum of one year upwards to three years), computer models are often implemented to reduce the time needed for evaluation and to supplement the information available.

The prevalence of numerical wind resource modeling has been on the rise due to computing advances, increased reliability, and the reduced costs over physical measurements. Implementing numerical techniques can reduce the need for physical measurements and can vastly shorten the time needed to estimate a wind resource (9). CFD and large scale NWP models are becoming more prevalent in wind resource assessment. The two techniques differ drastically in scale, resolution, solution techniques, and physical variables, but both provide useful results to wind developers. CFD and NWP models are both used to predict wind flow patterns, but over different time and spatial scales. NWP models use physical models to describe the air motions in the atmosphere over a very large spatial extent (hundreds to thousands of kilometers), and are tied to an extensive historical data set maintained in the U.S. by the National Center for Environmental Prediction (NCEP). Thus, when using an NWP model for a historical period of time, as is typically done for wind energy assessment, the NWP model has the distinct advantage of constantly correcting to the historical weather patterns. The spatial resolution of these boundary conditions are 1 degree (approximately 110 km), and this serves as limiting factor in the spatial resolution of NWP models. CFD codes do not generally have this advantage, and rely upon boundary condition data from field measurements or possibly from an NWP model. Furthermore, CFD may not model well the important energy fluxes at the earth's surface that define the atmospheric boundary layer, is computationally intensive due to its high spatial resolution, and presently is best at identifying terrain induced flow patterns under specific input flow conditions. Thus, for long term site assessment, mesoscale modeling is the computational tool of choice whereas CFD is used for identifying smaller scale flow patterns not resolved by lower resolution mesoscale models.

Site assessment in complex terrain is becoming increasingly important due to the rapid expansion of wind power into this type of terrain, and is of concern to wind developers and research institutes alike. Researchers from the National Weather Service in Reno, NV found that increasing the horizontal grid resolution in their study to three km made it possible to capture high wind speed events in the terrain near Reno, NV (10). The results obtained from this study corroborate well with a similar study that was conducted to determine how low level jet streams are affected by the terrain of Greenland (11). The authors of these studies concluded that increasing the horizontal resolution near complex terrain produced more accurate wind speed predictions. These papers did not address the affects of outer domain influence on wind speed predictions. It is the purpose of this study to demonstrate how MM5 predicts terrain induced wind flow and what type of domain simulation resolution and study area are required to produce accurate results.

The Pennsylvania State University/National Center for Atmospheric Research (PSU/NCAR) mesoscale model (known as MM5) is a limited area, non-hydrostatic model designed to simulate or predict mesoscale and regional-scale atmospheric circulation (12). MM5 has been used extensively by meteorologists, atmospheric scientists, and engineers to simulate the atmosphere for a number of different purposes. Due to the wide range of parameters computed by the model, MM5 has been used for a number of different applications, including studies done to determine environmental air quality (13), (14), validation of temperature cycles (15), and a study of solar radiation on Earth's surface (16), among many others. Each model simulation requires selection of the grid size and corresponding resolution (horizontal, vertical, and temporal) which influences the model's results. It has been shown that increasing the horizontal resolution of the MM5 solver improves the accuracy of the numerical results and provides improved predictions over more coarse resolution simulations (17). This conclusion is important to the current work as it dictated the grid resolutions selected and established an expectation for the results. Determine

Understanding how complex terrain has an affect on the wind flow is of interest to the research group as it may govern the feasibility of wind energy. The atmospheric boundary layer (ABL) is of great importance to those interested in wind energy, as all wind turbines are operated within it and as previously mentioned, determining the wind regime within the ABL, especially in complex terrain can be difficult and requires extensive computing resources. It is important to specify the size of model domain that will produce accurate results while reducing the need for computational resources. In this study, MM5 has been used to simulate the atmospheric state at a proposed wind development site with particular focus on the ABL. The numerical results obtained from MM5 were compared to the actual wind speed and direction measured at a meteorological tower installed at the site and used to determine the expected wind power density at the investigation site. This paper summarizes the domain influence comparison along with comparisons to experimental data. Results from two gridding scenarios were used for comparison to determine the necessity of an expanded outer domain. The details of these simulations and their results are explained within this paper.

AUBREY CLIFFS, AZ EXPERIMENTAL DATA

Experimental data has been collected as a part of an ongoing study through the Sustainable Energy Solutions (SES) group at Northern Arizona University (NAU)[1]. The proposed research site is located near Seligman, AZ and is owned in part by the state of Arizona and by the Navajo Nation. The site currently has five 30-meter meteorological towers and one 50-meter tower measuring the wind speed, direction, temperature, and pressure. The towers are owned, maintained, and operated by NAU. The first tower that was installed at the site is located at latitude N 035° 29.493' and longitude W 112° 59.463' and has been collecting data since June 2005. This location was used as the center of the numerical grid domain for a series of MM5 simulations and was the focus of this investigation. Approximately four years of data has been collected at this site along with about two years of data at tower sites within 10km of this initial location. The group currently has wind data for many locations in Arizona that is made publicly available through the web.

MODEL DESCRIPTION AND CONFIGURATION

MM5 is the latest version of this NWP model to be developed in unison with the model used by Anthes from PSU to simulate hurricanes and storm propagation (18). MM5 has played an important role in mesoscale meteorological research and the advancement of mesoscale NWP. The software package is comprised of a series of modular programs that define, prepare and run the model simulation. The first module used in MM5 is TERRAIN. This program horizontally interpolates and analyzes the latitude, longitude, and terrain height onto the chosen grid type. The grid type used for this study was the Lambert-conformal map projection. Two grid scenarios were developed with similar dimensions and resolutions to allow for direct comparison. The two scenarios are comparable in their horizontal and vertical resolutions but differ in the number of nested grid used. The first grid scenario used an outer domain size of 1116km x 1521km (North/South, East/West) with two nested domains each with size 246km x 219km and 52km x 52km for the second and third domains, respectively. The second grid scenario used the same dimensions as the inner two grids of scenario 1 but with no large outer domain. A map with both domain scenarios is shown in Fig. 1. The horizontal resolution used in the simulation is as follows: 9km for the outer most domain, 3km for the first nested domain, and 1km for the second nested domain. Both scenarios have 34 vertical levels of constant pressure ratio (denoted as sigma levels), with increased resolution in the ABL. In the ABL, which is generally between 300-m and 1000-m in height above the surface of the ground, the sigma levels were chosen to produce data at heights above the ground similar to those where data was collected at the experimental site (10-m and 30-m). The spacing of sigma levels within and directly above the ABL were chosen to facilitate proper communication of information (mass, momentum, and energy fluxes) to and from the ABL. The chosen sigma level variation is given in Table 1 along with the approximate height above sea level. It should be noted that the terrain modeled within inner most domain is considered highly complex (containing a steep escarpment). According to (10) MM5 is capable of modeling the complex, mountainous terrain that is subject of this study. Figure 2 shows the topography of the Aubrey Cliffs area. As can be seen, a large escarpment is present, rising about 400-m above the valley floor to its west. The prevailing wind direction is from the southwest at this location, so one would expect flow acceleration as the wind ascends up and over the cliff, and a turbulent separation pocket sometimes present near the edge of the cliff.

[1] www.ses.nau.edu (last accessed on January 8, 2010)

Table 1: Vertical resolution that was used for both model scenarios. Notice the increased resolution in the ABL.

Pressure Level	Sigma Value	Approximate Height Above Sea Level (m)
33	0.998	1,683
32	0.996	1,696
31	0.994	1,710
30	0.992	1,724
29	0.99	1.74E+03
28	0.988	1.75E+03
27	0.985	1.78E+03
26	0.98	1.82E+03
25	0.975	1.85E+03
24	0.97	1.89E+03
23	0.965	1.92E+03
22	0.96	1.97E+03
21	0.95	2.04E+03
20	0.94	2.11E+03
19	0.93	2.19E+03
18	0.92	2.29E+03
17	0.9	2.44E+03
16	0.88	2.63E+03
15	0.85	2.93E+03
14	0.8	3.33E+03
13	0.75	3.74E+03
12	0.7	4.17E+03
11	0.65	4.63E+03
10	0.6	5.11E+03
9	0.55	5.62E+03
8	0.5	6.15E+03
7	0.45	6.73E+03
6	0.4	7.34E+03
5	0.35	8.01E+03
4	0.3	8.73E+03
3	0.25	9.52E+03
2	0.2	1.09E+04
1	0.1	1.32E+04

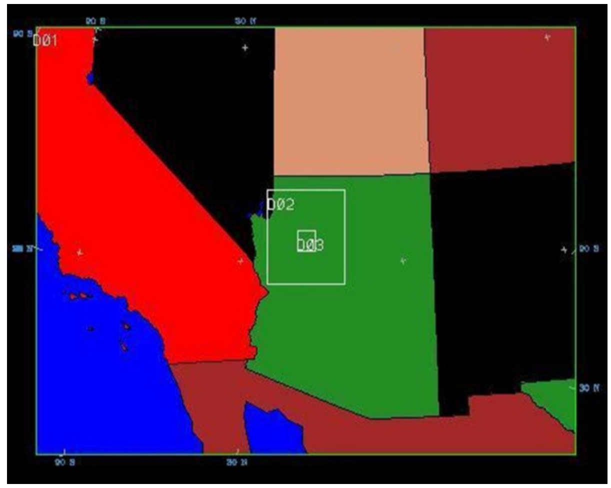

Figure 1: The map shows the domain extents used as inputs to the MM5 solver. The outermost (largest) domain used in scenario 1 is represented by the entire area depicted, with its nested two inner domains portrayed by smaller white rectangles labeled "D02" and "D03." In scenario 2, only the two inner domains were modeled.

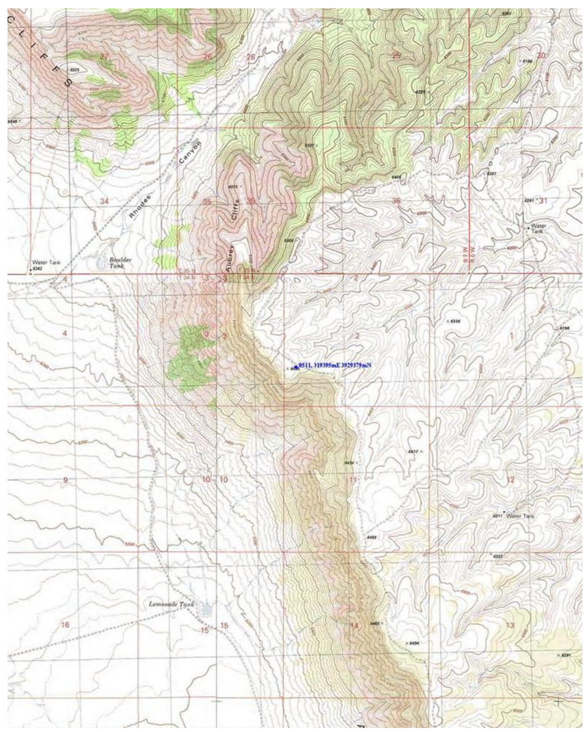

Figure 2: Topographic map of Aubrey Cliffs, AZ region. The meteorological station (marked in blue text) is approximately 100 m west of the nearest grid point. The area depicted in this map is entirely contained within the innermost modeling domain of both scenarios.

Once the two dimensional horizontal grid is created, the second module in MM5, REGRID reads in gridded meteorological data and interpolates it to constant pressure levels on the computational grid being employed in the simulation. For a given model run, all of the horizontal and vertical grid points are assigned meteorological data with some given temporal resolution to be used as the initial and boundary conditions. The data used for this model was obtained from the NCEP FNL[2] model in a six hour temporal resolution and 1.0° x 1.0° horizontal resolution. This data is then prepared for the model simulation by using the module in MM5, INTERPF to vertically interpolate data onto levels of constant reference state sigma, given by Eq. 1.

$$\sigma_k = \frac{P_{ijk} - P_{top}}{P^*_{ij}} \tag{1}$$

The reference state sigma level is defined by the hydrostatic pressure, P_{ijk}, the model's top level pressure, P_{top}, and the difference between the two dimensional surface pressure and the top pressure, P^*_{ij}. The initial and boundary condition data are read into MM5 which then solves for the unknown atmospheric variables (wind speed, temperature, pressure, etc.) using a non-linear mathematical model based upon the governing physics as explained by Grell and Dudhia (19). MM5 uses second-order, centered, finite difference and the second-order leap frog technique to solve the time variant atmospheric pressure equation, three dimensional momentum equations, and thermodynamic equation. Further information about the model description can be found at http://www.mmm.ucar.edu. Model scenario 1 was run for three one-month simulations and scenario 2 was run for one three-month simulation. It was necessary to break up model scenario 1 into three separate simulations due to the large amount of memory required for computation on the computing cluster available. It is assumed that the model scenarios are still comparable because the MM5 model updates the boundary conditions in 6-hour intervals to properly initialize the calculations. The outputs obtained from MM5 were saved in 10-minute time steps to gain significant temporal resolution for comparison.

MODEL OUTPUTS AND COMPARISON

The outputs from MM5 for both domain scenarios were compared for simulations that covered the first three months of 2006. The model grid point in each domain nearest to the meteorological tower was compared with the anemometer data for this period. The comparisons that were made were chosen to include the parameters that directly affect wind power generation. The wind speed and wind direction were compared at two heights above the ground near the anemometer location. The sigma level inputs to the model were used to calculate the altitude of the pressure surface above sea level via Eq. 2.

$$Z = -\frac{RA}{2g}\left(ln\frac{p_0}{p_{00}}\right)^2 - \frac{RT_{s0}}{g}\left(ln\frac{p_0}{p_{00}}\right) \tag{2}$$

Here, R is the universal gas constant, A is the adiabatic lapse rate, taken to be 50K/km, g is gravitational acceleration (9.81 m/s^2), T_{s0} is the reference surface temperature, taken to be 275K, p_0 is the surface level pressure, and p_{00} is the sea level pressure (10^5 Pa). As shown in Table 1, the sigma values of 1.0 and 0.996 resulted in heights above ground level (AGL) of 6.5m and 33m respectively. The two heights were compared with experimental data at heights of 10m and 30m, where cup anemometers were mounted on the meteorological tower. A comparison of the 10-minute average values found at these heights was completed to gain a better understanding of the overall model prediction capability.

To determine how well each of the data sets compares with the experimental data, the following statistical measures were computed:

Bias error, $$\bar{\phi} = \frac{1}{N}\sum_{i=1}^{N} \phi_i \tag{3}$$

Root mean square error,

$$\text{RSME} = \left[\frac{1}{N-1}\sum_{i=1}^{N}\left(\phi_i\right)^2\right]^{0.5} \tag{4}$$

Standard deviation of errors,

$$\text{SDE} = \left[\frac{1}{N-1}\sum_{i=1}^{N}\left(\phi_i - \bar{\phi}\right)^2\right]^{0.5} \tag{5}$$

Where $\phi_i$is defined as the difference between the model and experimental variable, and N is the total number of observations, 12690 (equal to the number of 10 minute periods in three months). The errors computed include contributions from systematic and nonsystematic sources. Systematic errors consist of a bias in the model which is usually caused by errors in topography, physical parameters, or numerical computation. Nonsystematic errors, which are indicated by the standard deviation error, represent uncertainties in the model boundary conditions or errors in observations (20).

The expected wind power density (WPD) from the test site was also computed by using the air density, which was found from the model pressure and temperature using the ideal gas law for dry air given by Eq. 6.

[2]National Center for Environmental Prediction (NCEP) http://dss.ucar.edu/datasets/ds083.2/ Accessed 2009

$$\rho = \frac{P}{R*T} * 1000 \quad (6)$$

Where ρ is given in kg/m^3, P is the total pressure in kPa, R is the universal gas constant, and T is the temperature in K. Using the computed density from the model and the 10-minute average magnitude of the wind velocity, the WPD was computed using the relationship shown by Manwell et. al. (1) and stated by Eq. 7.

$$WPD = {}^{1}/_{2}\,\rho V^{3} \quad (7)$$

Here, WPD has units of W/m^2, ρ is given by Eq. 6, and V is the magnitude of the 10-minute average wind speed.

The model simulations that were completed include two separate runs using model scenarios 1 and 2, each of which simulate the first three months of 2006. A summary of each of the runs and their specific attributes is given in Table 2.

Table 2: Summary of model simulations conducted for comparison.

Scenario	Number of Domains	Horizontal Resolution	Vertical Resolution	Length of Run
1	3	9km, 3km, 1km	34 sigma levels	3 one month runs
2	2	3km, 1km	34 sigma levels	3 consec-utive months

RESULTS AND DISCUSSION

During the first three months of 2006 the wind speed magnitude and general trend of the experimental data were estimated well by both model scenarios. The model predicted the magnitude of high wind speed events but did not always predict the correct time they occurred. The average wind speed from the experimental data was found to be 7.86 m/s. Model scenario 1 predicted the average wind speed to be 7.38 m/s and model scenario 2 predicted 7.55 m/s. This corresponds to a 6.1% error and 3.9% error for scenario 1 and 2, respectively. Although the percent difference is low, this error will be emphasized when considering the wind speed cubed. The average wind direction was also calculated for the first three months of 2006 for comparison. Again, the model predicts the experimental data accurately. The meteorological tower data estimates that the average wind direction was 166°. Model scenario 1 predicted an average of 171°, while the average from scenario 2 was found to be 159°. The distribution of wind speeds for model scenario 1 and the experimental data were used to produce a wind rose. The wind rose shows the predominant wind directions and the frequency of the corresponding wind speeds from these directions. These plots are shown in Fig. 3. The six-hour average of the wind speed for the month of January 2006 at 10m AGL and 30m AGL is shown in Figs. 4 and 5. Figure 6 shows the three data sets for the entire three month simulation period at the 30m AGL location. The model was not able to correctly estimate the magnitude of the high wind speed event that occurred within the first 48 hours of the simulation. This could be attributed to the model start up time needed to allow the boundary conditions to correctly resolve the atmosphere. To gain better perspective at how well the model predicts the experimental data, multiple correlation coefficients were calculated. The correlation coefficients were calculated for individual months to reduce the effects introduced by temporal inaccuracies. For model scenario 1, the 10-minute averaged correlation coefficient for the month of January was computed to be 0.556. The hour, six-hour, and 24-hour average correlation coefficients were found to be, 0.569, 0.623, and 0.772, respectively. During the month of January, model scenario 2 produced similar results with the 10-minute, hour, 6-hour, and 24-hour correlation coefficients found to be, 0.536, 0.545, 0.593, 0.752, respectively. The increasing values of correlation coefficients demonstrate that as the predicted wind speeds are averaged over time, the results more closely approximate the experimental data. The remaining two months of simulation data contributed to considerably lower computed correlation coefficients. It was found that model scenario 1, when all three months of data were used for correlation, the coefficient was 0.297. This poor correlation is attributed to the simulation predicting wind speeds at incorrect times. During February and March, both model scenarios falsely predicted the occurrence of high wind speed events. The results show that model scenario 1 lagged behind the experimental results by 10-20 hours, while scenario 2 lagged by approximately 8-10 hours. As shown in Table 2, model scenario 2 was simulated for the entire three-month period in one computational run, without re-initializing the MM5 solver. This suggests that continuous simulations will more accurately predict the atmospheric conditions.

The simulation data and the experimental data for the entire three month period were compared using the statistical measures mentioned previously, summarized in Table 3. It was found that the mean bias error at 30m was -0.48 and -0.29 domain scenario1 and 2, respectively. The 10m location had a greater deviation from the experimental data. This is attributed partly to the 3.5m difference between the model and actual heights, and the inherent difficulty in prediction of the wind speed at such a low height AGL. It was found that the root mean square error and standard deviation of the errors was considerably high. The RMSE and the SDE tend to put a greater emphasis on values that are further from the expected wind speed. This may represent errors in the boundary conditions that propagate into the model simulation. These non-systematic errors also may be attributed to uncertainties in the experimental data. It is also difficult to be confident in the ability of the model to properly predict high wind speed events at the correct time. A portion of the bias error incurred in the simulation may have developed due to the horizontal resolution that represents the topography. The 1-km resolution does not completely define the steep elevation gain at the cliff and introduces a bias error that reduces the accuracy of the results.

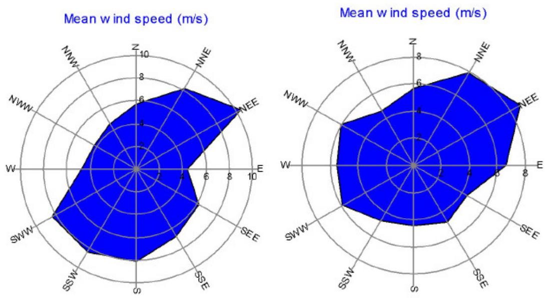

Figure 3: Wind rose comparison of the experimental data (left) and model scenario 1 prediction (right).

Table 3: Computed error between model scenarios and experimental values for 10m and 30m AGL.

Model Scenario	Average Wind Speed	Bias Error	RMSE	SDE
Scenario 1 at 30 m AGL	7.38 m/s	-0.48 m/s	5.49 m/s	5.47 m/s
Scenario 1 at 10 m AGL	5.23 m/s	-0.87 m/s	4.1 m/s	3.9 m/s
Scenario 2 at 30 m AGL	7.55 m/s	-0.29 m/s	4.73 m/s	4.72 m/s
Scenario 2 at 10 m AGL	5.48 m/s	-0.58 m/s	3.77 m/s	3.72 m/s

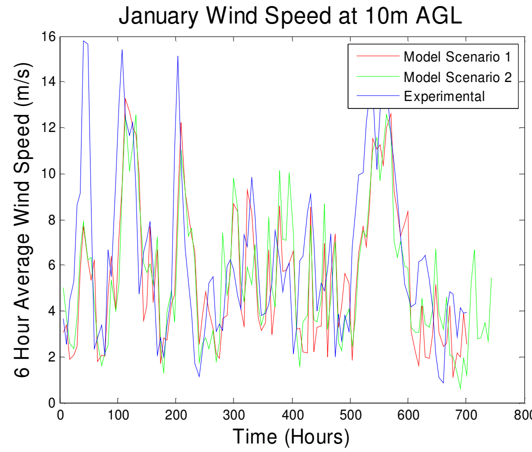

Figure 4: Six-hour average of the wind speed for the month of January 2006 at 10 meters AGL. The model accurately predicts high wind speed events and the general trend of the wind speed at the meteorological tower.

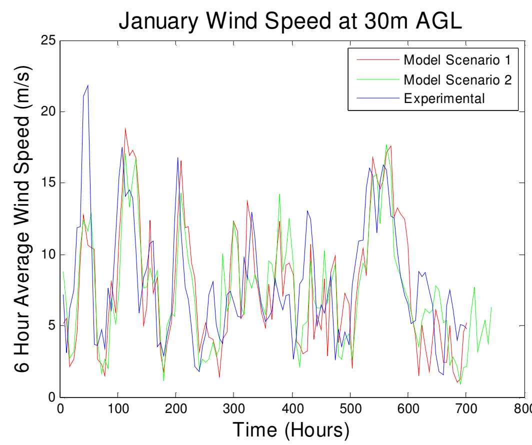

Figure 5: Six-hour average of the wind speed for the month of January 2006 at 30 meters AGL.

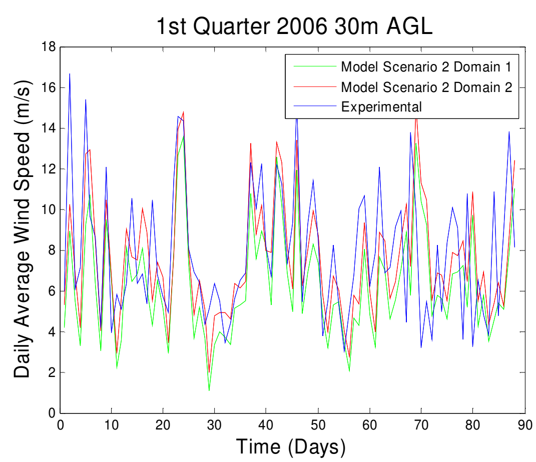

Figure 6: Time-series plot of the 24-hour average wind speed prediction from both model scenarios and the meteorological tower data at 30m AGL.

The mean WPD at 30m AGL was computed for the experimental data, model scenario 1, and model scenario 2. The air density was computed from the model pressure and temperature using Eqn. 6. The average air densities computed from the model are 1.0303 kg/m^3 and 1.0106 kg/m^3 for scenario 1 and 2, respectively. Scenario 1 differs from the experimental data by 3.0% while scenario 2 differs by 1.1%. The air density is plotted for the each model over the three-moth simulation period in Fig. 7. The illustration shows that the models predicted the experimental air density variation well, but with a slight bias error. Using the experimental calculated air density, the average WPD of the experimental data was found to be 483 W/m^2. The model predicted considerably lower values, with scenario 1 having a mean WPD of 435 W/m^2 and scenario 2 having a mean WPD of 395 W/m^2. As previously noted, the difference found in the computed wind speeds is emphasized by the cubic WPD formulation. In Fig. 8 the WPD is plotted against time to demonstrate how the model differs from the experimental data. Figures 8 and 9 show the WPD during the month of January at 10m and 30m AGL, respectively. Many of the high wind speed events are simulated by the model to occur at times after the actual event. Again, there does seem to be some discrepancy during the model start up time.

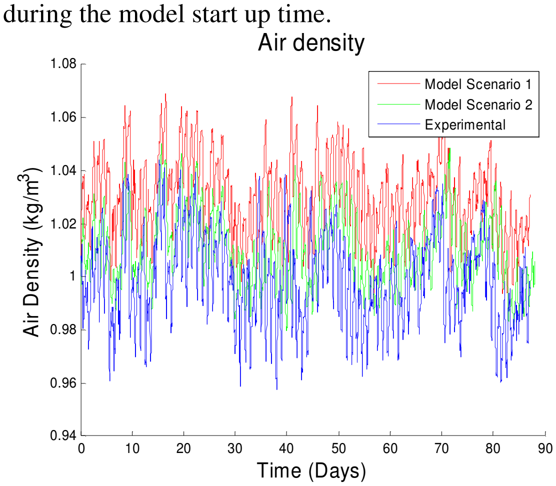

Figure 7: Air density found at the test site during the first quarter of 2006. The plot shows a 1-3% difference in actual air density versus experimental air density.

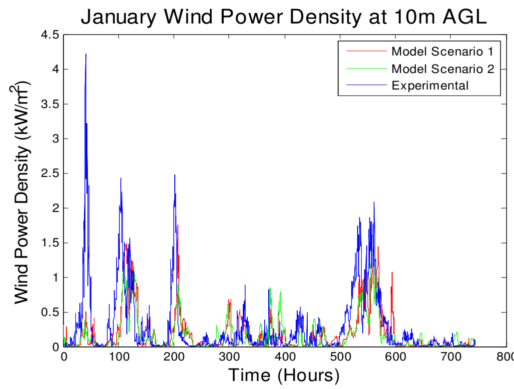

Figure 8: Wind power density at the test site during January 2006 at 10m AGL. Note the similarity in the timing of high wind speeds.

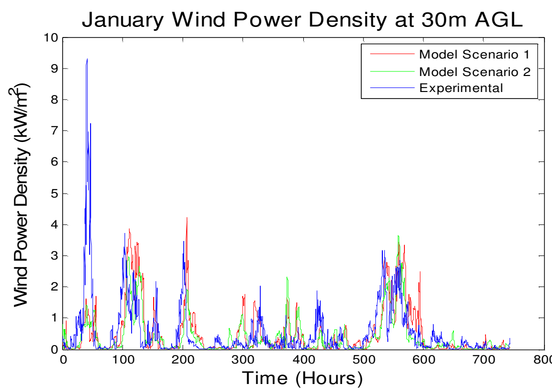

Figure 9: Wind power density at the test site during January 2006 at 30m AGL.

The terrain at Aubrey Cliffs and the prevailing wind direction suggest that the atmospheric flow will accelerate as it moves up and over the cliffs. The MM5 results show this to be true as seen in the wind speed vector map displayed in Fig. 10. This figure shows the velocity vectors in the ABL displayed in a global color scale representing wind speed. The length and direction of the arrows represent the magnitude of the wind velocity. The ground is represented by gray scale, with lighter regions representing higher elevations. It can be seen that in the center of the figure, the light region represents the cliff face. This figure was generated using model scenario 2 and shows the three month average of the data. Computing the average gives a better interpretation of how the air moves within the region. For instance, the vertical wind profile within the lowest 100m of the ABL decreases in velocity and becomes inverted as it approaches the cliffs from the south-southwest. As the air moves up and over the cliff face, it accelerates and eventually conforms to a more laminar, stable boundary layer profile. It can be seen that the wind flow re-circulates in the valley west of the cliff. This causes the southwesterly flow of wind in the valley to be less, which can be confirmed by comparison to meteorological data taken in Aubrey Valley. The average wind speed within the valley for the first three months of 2006 was found to be 3.09 m/s, which is considerably lower than the value of 8.07 m/s previously noted at the top of the cliff.

Visual representations of the horizontal wind speed were also generated using the MM5 data. Figure 11 shows the magnitude of the wind velocity at 6.5 meters (top) and 33 meters (bottom) AGL. These "wind maps" were created from the average wind velocity found over three months generated from MM5 model scenario 2. The maps confirm the acceleration of the wind as it moves past the cliff face, and also show areas of high wind speed that would be of interest to wind developers. The ability to produce these maps with the mesoscale wind data allows wind developers to understand and quantify the wind speed for any proposed wind development site.

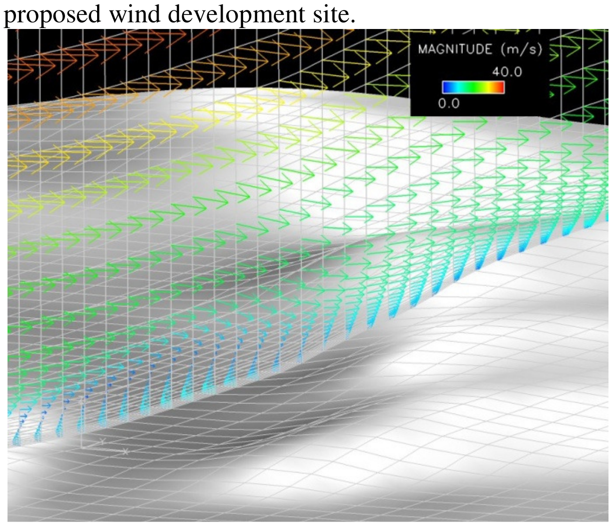

Figure 10: Visual representation of ABL from the results produced in MM5. The images show how the boundary layer is altered by the topography in proximity to the cliff. The ABL is shown to be unstable with separated flow patterns as it approaches the cliffs (top)

The results demonstrate that MM5 simulated the variables related to wind energy with high accuracy. Additional work needs to be done to better understand the simulation lag in predicting high wind speed events. The differences between scenario 1 and scenario 2 do not suggest that the outer domain will drastically affect the simulation results. For this reason, and the increased computational resource needed for its use, it is recommended that the smaller grid scenario be implemented for future runs. It may be possible that other weather phenomenon will be different if a larger outer domain is used. Storm propagation, precipitation, humidity, and other atmospheric variables may be altered by the influence of the outer domain.

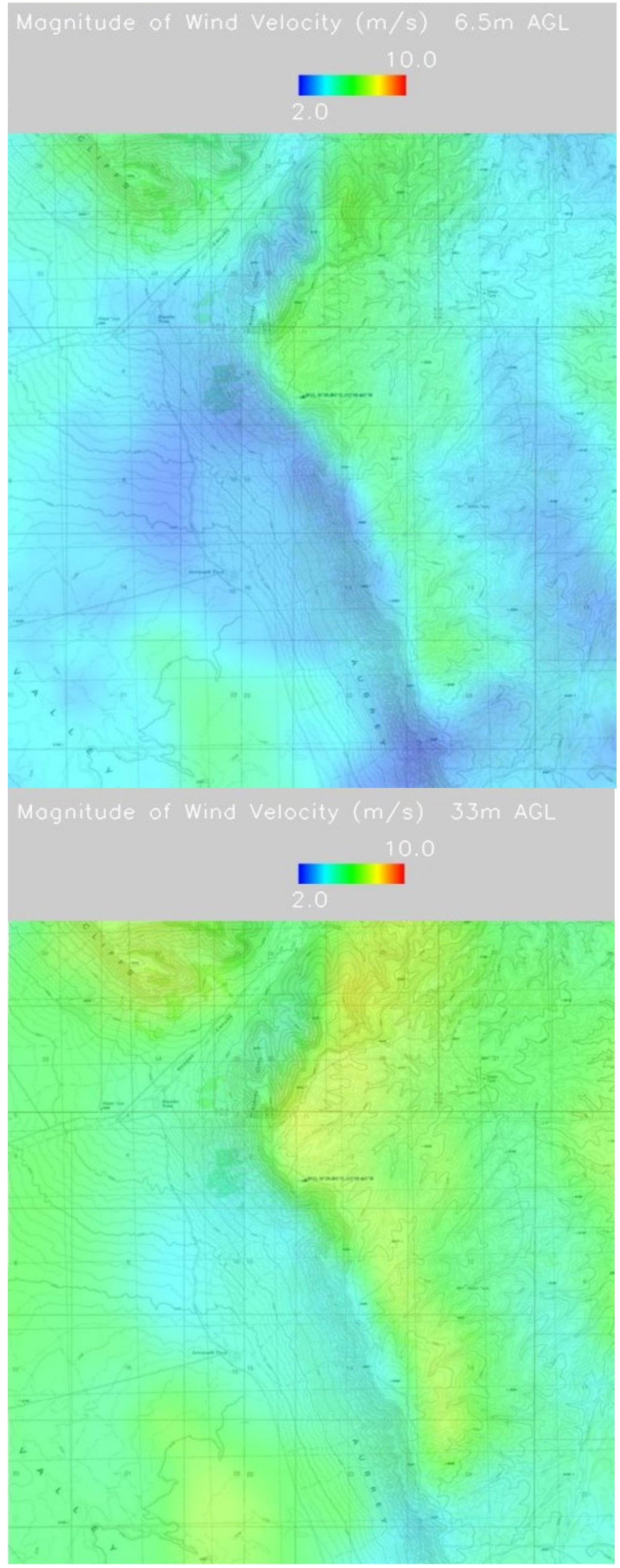

Figure 11: Wind speed map at Aubrey Cliffs. The 3-month averaged wind velocity is shown at 6.5m AGL (top) and 33M AGL (bottom).

CONCLUSION AND SUMMARY

It was found that the MM5 model accurately predicts the wind speed at the meteorological test site, particularly during the first month of the simulation. The model does a good job estimating the trend of high speed events, but lags behind the actual occurrence. The results also demonstrated that accurate predictions of WPD and the prevailing wind direction can be made using MM5. This outcome demonstrates that using the model to evaluate a wind site would be beneficial to wind developers. The bias error in the model can be corrected to give the developer a very accurate value of the site's capacity factor. It was found that there are no considerable differences in predicting wind speeds when a larger outer domain is used in the model. Although the wind speed estimations were similar for both domain scenarios, it was shown that other meteorological variables were not affected by the influence of the outer domain. The smaller domain scenario is still able to capture synoptic scale storms and weather patterns that may develop.

The simulations described in this paper will be used in future analysis when more numerical data is available. One goal of the current research team is to generate long term numerical wind characteristics that can be used for additional comparisons at other anemometer locations to further validate the outcomes from this paper.

REFERENCES

1. **Manwell, J. G., McGowan, Jon and Rogers, Anthony.** *Wind Energy Explained Theory, Design and Application.* West Sussex PO19 8SQ, England : John Wiley & Sons Ltd., 2002.

2. **AWS Scientific, Inc.** *Wind Resource Assessment Handbook.* Albany, NY : CESTM, 251 Fuller Road, 1997.

3. **Pérez, S. et al.** Using the MM5 model for wind prediction in a complex terrain site. 2003.

4. **Marti, I.** Wind power prediction in complex terrain: from the synoptic scale to the local scale. 2004.

5. **Jimenez, Barbara.** Offshore Wind Resource Assessment with WAsP and MM5: Comparative Study for the German Bight. 2007, pp. 121–134.

6. **Frank, Helmut P., Rathmann, Ole and Mortensen, Niels G.** *The Numerical Wind Atlas the KAMM/WAsP Method.* Roskilde, Denmark : Risø National Laboratory, 2001.

7. **Villanueva, J. and Martí, I.** Improving wind resource assessment and wind forecast by using a CFD model developed in CENER. 2004.

8. **NRG.** NRG-NOW System 50m XHD Calibrated SymphoniePLUS™, with 2.4m Booms. [Online] October 26, 2009. http://www.nrgsystems.com/.

9. **Alexandre, Costa, et al.** A review on the young history of the wind power short-term prediction. 2008, pp. 1725–1744.

10. **Cairns, M. and Corey, J.** Mesoscale Model Simulations of High-Wind Events in the Complex Terrain of Western Nevada. 2003, pp. 249-263.

11. **Doyle, James D. and Shapiro, Melvyn A.** *Flow Response to Large-Scale Topography: The Greenland Tip Jet.* Monterey, CA : Naval Research Laboratory, 1998.

12. **UCAR.** University Corporation for Atmospheric Research. *MM5 Community Model.* [Online] 2005. http://www.mmm.ucar.edu/mm5/.

13. **Grineski, Sara and Bolin, Bob.** Criteria Air Pollution and Marginalized Populations: Environmental Inequity in Phoenix, Arizona. 2007, pp. Volume 88, Number 2.

14. **Zehnder, Joseph A.** Simple Modifications to Improve Fifth-Generation Pennsylvania State University–National Center for Atmospheric Research Mesoscale Model Performance for the Phoenix, Arizona, Metropolitan Area. 2002, pp. 971–979.

15. **A. Brazel, Susanne Grossman-Clarke, Joseph A. Zehnder, Brent C. Hedquist.** *OBSERVATIONS AND MM5 SIMULATIONS OF THE URBAN HEAT ISLAND IN PHOENIX, ARIZONA, USA WITH A MODIFIED LAND COVER SCHEME.* Phoenix, AZ : Arizona State University.

16. **Yang, Kun.** Estimating surface solar radiation from upper-air humidity. 2002, pp. 177-186.

17. **Mass, Clifford F. and Ovens, David.** *DOES INCREASING HORIZONTAL RESOLUTION PRODUCE MORE SKILLFUL FORECASTS?* Seattle, WA : American Meteorological Society, 2001.

18. **Anthes, R. and Warner, T.** Development of Hydrodynamic Models Suitable for Air Pollution and Other Mesometerological Studies. 1978, pp. 1045–1078.

19. **Grell, Georg and Dudhia, Jimy.** *A Description of the Fifth-Generation Penn State/NCAR Mesoscale Model (MM5).* s.l. : NATIONAL CENTER FOR ATMOSPHERIC RESEARCH, 1994.

20. **Zhong, F and Fast, J.** An Evaluation of the MM5, RAMS, and Meso-Eta Models at Subkilometer Resolution Using VTMX Field Campaign Data in the Salt Lake Valley. 2003, pp. 1301-1322.

21. **Moore, K and Bailey, B.** *Maximizing the Accuracy of Sodar Measurements.* s.l. : AWS Truewind, August 2006.

22. **Kuo, Bill.** UCAR/MMM. *www.ucar.edu/governance/meetings/oct04/followup/basc/Kuo.pdf.* [Online] 2004.

23. **Jackobson, M.** *Fundamentals of Atmospheric Modeling 2nd Edition.* Cambridge, NY : Cambridge University Press, 2005.

24. **Helmut P. Frank, Ole Rathmann, Niels G. Mortensen, Lars Landberg.** *The Numerical Wind Atlas the KAMM/WASP Method.* Roskilde, Denmark : Risø National Laboratory, 2001.
25. **Bitsuamlak, G. T., Stathopoulos, T and Bédard, C.** Numerical Evaluation of Wind Flow over Complex Terrain:. 2004, pp. 135-145.
26. **Hargreaves, D.M and Wright, N.G.** On the use of the k–ε model in commercial. 2007, pp. 355-369.
27. **McNerney, G. and Veers, P.** A Markov Method for Simulating Non-Gaussian Wind Speed Time Series. January 1985.
28. **Richards, P.J. and Hoxey, R.P.** Appropriate boundary conditions for computational wind engineering models using the k-E turbulence model. 1993, pp. 145-153.